Griffiths phase and critical behavior of the 2D Potts models with long-range correlated disorder

Christophe Chatelain

Griffiths phase and critical behavior of the 2D Potts models with long-range correlated disorder

Christophe Chatelain
Groupe de Physique Statistique, Département P2M,
Institut Jean Lamour (CNRS UMR 7198), Université de Lorraine, France
(Dated: August 3, 2013)

The q-state Potts model with a long-range correlated disorder is studied by means of large-scale Monte Carlo simulations for $q = 2, 4, 8$ and 16. Evidence is given of the existence of a Griffiths phase, where the thermodynamic quantities display an algebraic Finite-Size Scaling, in a finite range of temperatures around the self-dual point. The critical exponents are shown to depend on both the temperature and the exponent of the algebraic decay of disorder correlations, but not on the number of states of the Potts model. The mechanism leading to the violation of hyperscaling relations is observed in the entire Griffiths phase.

PACS numbers: PACS numbers: 64.60.De, 05.50.+q, 05.70.Jk, 05.10.Ln

I. INTRODUCTION

It is well known that the presence of impurities can greatly affect the properties of a physical system, especially when the latter undergoes a phase transition. In the following, the case of frozen impurities, i.e. quenched disorder, coupled to the energy density of the system is considered. It is assumed that no frustration is induced by randomness. With these assumptions, Harris analyzed the conditions for a change of critical behavior at a second-order phase transition upon the introduction of disorder [1]. In the language of Renormalization Group (RG), disorder is a relevant perturbation when its fluctuations in a finite domain grow faster than the fluctuations of the energy, or equivalently, when the specific heat exponent α of the pure model is positive. On the theoretical side, the q-state Potts model provides a useful and simple toy model to study the influence of disorder. In two dimensions, the pure model undergoes a second-order phase transition when $q \leq 4$ with a q-dependent universality class. Upon the introduction of quenched disorder, the critical behavior is governed by a new q-dependent RG fixed point when $2 < q \leq 4$. A good agreement between numerical calculations [2] and RG series expansions [3] of the critical exponents has been achieved. In the case $q = 2$, equivalent to the Ising model, disorder is a marginally irrelevant perturbation and the critical behavior is only modified by multiplicative logarithmic corrections [4]. In the three-dimensional case, only the Ising model undergoes a second-order phase transition. As predicted by the Harris criterion, a new critical behavior is found by RG studies and observed numerically [5].

When the pure system undergoes a first-order phase transition, the introduction of disorder softens the energy jump and reduces the latent heat [6]. For a strong enough disorder, a continuous phase transition can be induced. In two dimensions, an infinitesimal amount of disorder is sufficient to induce a second order phase transition [7, 8]. This rigorously-proved statement was first tested in the case of the 8-state Potts model [9]. In the entire regime $q > 4$, where a first-order phase transition is undergone by the pure Potts model, a continuous transition is induced with a q-dependent critical behavior [10]. In three dimensions, the softening of the transition was observed numerically for the $q = 3$ [11] and $q = 4$ [12] Potts models, as well as in the limit $q \to +\infty$ [13]. For weak disorder, the transition remains discontinuous, while at strong disorder, it becomes continuous.

It was implicitly assumed in the above discussion that the disorder was uncorrelated. This may not be the case anymore if the impurities interact and were given enough time to equilibrate. This situation may be encountered with charged impurities. At a second-order phase transition, long-range correlated disorder leads to a critical behavior that can be distinct from the case of short-range or uncorrelated disorder. Weinrib and Halperin studied by RG the n-component ϕ^4-model in dimension $d = 4-\epsilon$ with a correlated disorder decaying algebraically with an exponent $a = 4 - \delta$ [14]. In the same spirit as the Harris criterion, such a long-range correlated disorder is shown to be relevant when the correlation exponent ν of the pure model satisfies the inequality $\nu < 2/a$. Interestingly, disorder is a marginally irrelevant perturbation at the new long-range random fixed point, which means that $\nu = 2/a$. This relation was proved to be exact at all orders in perturbation [15] and was later confirmed by Monte Carlo simulations of the 3D Ising model [16] and an explicit RG calculation of the 2D Ising model [17].

Weinrib and Halperin calculation is based on the assumption that disorder correlations are isotropic and that n-point disorder cumulants are irrelevant for $n > 2$. Anisotropically correlated disorder is therefore out of its range of validity. The latter has attracted a lot of attention since the introduction of the celebrated McCoy-Wu model [19], which corresponds to an Ising model with randomly distributed couplings J_1 and J_2 in one direction and infinitely correlated in the second

direction of the square lattice [19]. While planar defects lead to a smearing of the transition of the 3D Ising model [18], the phase transition of this 2D Ising model with parallel linear defects remains sharp. Exploiting the mapping to the Ising quantum chain in a transverse field, the critical exponents of the McCoy-Wu model were determined exactly: $\beta = (3-\sqrt{5})/2$ and $\nu = 2$ [20]. When algebraically decaying disorder correlations are introduced in the transverse direction of the McCoy-Wu model, the Weinrib-Halperin law $\nu = 2/a$, where a is the disorder correlation exponent, is recovered [21]. Interestingly, the critical behavior of the Potts model with uncorrelated homogeneous disorder was conjectured to be described by an isotropic version of the McCoy-Wu-Fisher fixed point in the limit $q \to +\infty$ [23]. The McCoy-Wu model is the first model where a Griffiths phase was observed [24]. In a finite range of temperatures, the susceptibility diverges and the magnetization is singular. This phenomena is due to the existence of rare macroscopic regions with a high concentration of strong couplings that can order independently of the rest of the system [25]. The Griffiths phase should also be present in the aforementioned Potts models with isotropic disorder but it is believed to be too weak to be observed numerically. The McCoy-Wu model is easily extended to q-state Potts spins. In the regime $q \leq 4$, the critical behavior was proved to be independent of the number of states q and therefore identical to that of the original McCoy-Wu model [26]. Numerical calculations showed that the first-order phase transition of the Potts model with $q > 4$ is completely rounded, like in the case of homogeneous disorder, but, in contrast to homogeneous disorder, the critical behavior induced by disorder is independent of q and therefore described by the infinite-disorder McCoy-Wu-Fisher fixed point [27]. Different arrangements of correlated couplings were also studied. An aperiodic sequence of couplings J_1 and J_2 in one direction, infinitely correlated in the second direction of a square lattice, also provokes the rounding of the first-order phase transition of the Potts model when the wandering exponent of the sequence is sufficiently large [28]. However, in contrast to the McCoy-Wu model, the induced critical behavior depends on the number of states q.

Recently, we have studied the 2D 8-state Potts model with an isotropic correlated non-Gaussian disorder [29]. Such a disorder was obtained by simulating an Ashkin-Teller model on a critical line of its phase diagram. To each independent spin configuration is assigned a coupling configuration for the Potts model. We have shown by Monte Carlo simulations that the first-order phase transition of the 8-state Potts model is rounded. Disorder fluctuations are large and cause the violation of the hyperscaling relation, in the same way as in the 3D random-field Ising model, even though no frustration is present. In this work, we show that this behavior is actually observed in a finite range of temperatures and for all numbers of states q of the Potts model. The paper is organized as follows. Details of the model and the simulations are given in the first section. In the second section, the phase diagram is discussed and evidences are given of the existence of a Griffiths phase. The critical behavior at the self-dual point and in this Griffiths phase is presented in the third section. Non self-averaging properties and hyperscaling violation are finally discussed in the fourth section.

II. MODELS AND NUMERICAL DETAILS

The 2D q-state Potts model is defined by the Hamiltonian [30]

$$H = -\sum_{(i,j)} J_{ij}\delta_{\sigma_i,\sigma_j} \tag{1}$$

where the spins σ_i lie on the nodes of a square lattice and can take q possible values. The sum is restricted to pairs of nearest neighbors of the lattice. Note that the temperature is not absorbed in the definition of the couplings. We use the conventional order parameter m, called magnetization, defined as

$$m = \frac{q\rho_{\max.} - 1}{q-1} \tag{2}$$

where $\rho_{\max.}$ is the fraction of spins in the majority state. Thermodynamic quantities are generated by means of Monte Carlo simulations using the Swendsen-Wang cluster algorithm [31]. A total of 1393 Monte Carlo simulations were run, representing 25 years of CPU time.

In the following, the average over thermal fluctuations is denoted by brackets, for example $\langle m \rangle$ in the case of magnetization. Since the exchange couplings J_{ij} are quenched random variables, a further average over the probability distribution of these couplings is required. An over line is used to denote this average, as for example $\overline{\langle m \rangle}$ for the average magnetization. In order to generate the coupling configurations, an auxiliary isotropic Ashkin-Teller model is simulated. This model corresponds to two Ising models locally coupled by their energy density and is defined by the Hamiltonian [32]

$$-\beta H^{\mathrm{AT}} = \sum_{(i,j)} \left[J^{\mathrm{AT}}\sigma_i\sigma_j + J^{\mathrm{AT}}\tau_i\tau_j + K^{\mathrm{AT}}\sigma_i\sigma_j\tau_i\tau_j \right]. \tag{3}$$

This Hamiltonian is invariant under the reversal of all spins σ_i, all spins τ_i or both σ_i and τ_i. Two order parameters can be defined: magnetization $M = \langle |\sum_i \sigma_i| \rangle$ and polarization $P = \langle |\sum_i \sigma_i\tau_i| \rangle$. The phase diagram of the Ashkin-Teller model presents several lines separating a paramagnetic phase ($M = P = 0$), a Baxter phase where all spins are in the same state ($M, P \neq 0$) and a phase where each Ising replica is disordered but there exists order between them ($M = 0, P \neq 0$). The line

separating the paramagnetic and Baxter phases is given by self-duality arguments [33]:

$$e^{-2K} = \sinh 2J. \tag{4}$$

The critical exponents along this line were obtained through the conjecture of a mapping [34] of the Ashkin-Teller model onto an eight-vertex model exactly solved by Baxter. In terms of the parameter $y \in [0; 4/3]$ of the eight-vertex model and related to the couplings along the line by

$$\cos\frac{\pi y}{2} = \frac{1}{2}\left[e^{4K} - 1\right], \tag{5}$$

these critical exponents read

$$\beta_\sigma^{\mathrm{AT}} = \frac{2-y}{24-16y}, \quad \beta_{\sigma\tau}^{\mathrm{AT}} = \frac{1}{12-8y}, \quad \nu^{\mathrm{AT}} = \frac{2-y}{3-2y}. \tag{6}$$

Note that $\beta_\sigma^{\mathrm{AT}}/\nu^{\mathrm{AT}} = 1/8$ is constant while $\beta_{\sigma\tau}^{\mathrm{AT}}/\nu^{\mathrm{AT}}$ varies along the self-dual line. Therefore, polarization-polarization correlation functions decay algebraically

$$\langle \sigma_i\tau_i\sigma_j\tau_j\rangle \sim |\vec{r}_i - \vec{r}_j|^{-a} \tag{7}$$

with an exponent

$$a = 2\beta_{\sigma\tau}^{\mathrm{AT}}/\nu^{\mathrm{AT}} = \frac{1}{4-2y} \tag{8}$$

that can be tuned by moving along the critical line. In order to construct correlated coupling configurations for the Potts model, a set of typical spin configurations of the Ashkin-Teller model at different points of the self-dual line are first generated by Monte Carlo simulation. We used the cluster algorithm proposed by Salas and Sokal [35]. To each spin configuration is then associated a coupling configuration of the Potts model by

$$J_{ij} = \frac{J_1 + J_2}{2} + \frac{J_1 - J_2}{2}\sigma_i\tau_i \tag{9}$$

where the site j is located after the site i on the lattice, i.e. on its right or below. Because of this construction, disorder correlations $\overline{(J_{ij} - \bar{J})(J_{kl} - \bar{J})}$ decay algebraically with an exponent a that can be tuned. We have considered the six values $y \in \{0, 0.25, 0.50, 0.75, 1, 1.25\}$ corresponding to the exponents $a \simeq 0.25$, 0.286, 0.333, 0.4, 0.5 and 0.667. The two couplings J_1 and J_2 are chosen to be related by

$$\left(e^{J_1} - 1\right)\left(e^{J_2} - 1\right) = q \tag{10}$$

corresponding to the self-duality condition when $\beta = 1/k_BT = 1$. With this definition, the self-dual point is therefore located at $\beta_c = 1$. The strength of disorder is measured by the ratio $r = J_2/J_1$.

Note that, in the following, this disorder will be referred to as correlated disorder to distinguish it from uncorrelated disorder. However, it is important to keep in mind that, as described above, it was obtained using a very particular construction and does not display the same properties as the correlated disorder considered by Weinrib and Halperin. In the latter, disorder was indeed distributed according to a Gaussian probability distribution so that $2n$-point correlation functions are related to two-point correlations by the Wick theorem. This is not the case for the Ashkin-Teller model and, therefore, for the couplings that are generated from the typical spin configurations of this model.

III. TEMPERATURE DEPENDENCE

In this section, the temperature dependence of the average thermodynamic quantities is investigated to determine the phase diagram of the model. Note that the temperature affects only the Potts model and not the auxiliary Ashkin-Teller model used to construct the coupling configurations. Disorder correlations decay algebraically independently of the temperature. Two numbers of Potts states, $q = 2$ (equivalent to the Ising model) and $q = 8$, are considered. As mentioned in the introduction, the former undergoes a second-order phase transition in the absence of disorder while the latter displays a discontinuous transition. Monte Carlo simulations were performed for the lattice sizes $L = 32, 48, 64$ and 96. The exponent of the algebraic decay of the disorder correlations was fixed to $a = 0.4$, which corresponds to a parameter $y = 0.75$ for the auxiliary Ashkin-Teller model. For comparison, the case of an uncorrelated disorder is also considered and presented in an inset in each figure. The thermodynamic quantities were averaged over 14563 disorder configurations for $L = 96$, 32768 for $L = 64$, 58254 for $L = 48$ and 131072 for $L = 32$. For each disorder configuration, 2000 Monte Carlo iterations were performed to estimate the thermal averages. The case of the Ising model is first discussed.

A. Ising model

As can be observed on Fig. 1, the magnetization curve of the Ising model with correlated disorder is not typical. Instead of the usual single abrupt variation of magnetization, two such variations are seen. Between the paramagnetic and ferromagnetic phases, an intermediate region of slow variation is present. This behavior is remarkably different from the case of uncorrelated disorder shown in the inset. With correlated disorder, the magnetization displays a strong lattice-size dependence in the intermediate regime, similar to what is observed in the paramagnetic phase. As will be more extensively discussed in the next section, this behavior is algebraic. It is tempting to associate the boundaries of this intermediate regime to the two temperature scales introduced by the two Potts couplings J_1 and J_2. In the case presented here, these

two couplings are solutions of the self-duality condition (10) with $r = J_2/J_1 = 3$. Numerically, $J_1 \simeq 0.4812$ and $J_2 \simeq 1.4436$. Neighboring spins linked by strong couplings J_2 are preferably in the same state for inverse temperatures $\beta = \frac{1}{k_B T} \lesssim \frac{1}{J_2} \simeq 0.6927$. As can be seen on Fig. 1, a quick variation of magnetization is indeed observed around this temperature. Weak couplings introduce a second inverse temperature scale $\beta = \frac{1}{J_1} \simeq 2.079$ which is, in contrast, quite far from the second fast variation of magnetization which occurs already around $\beta \simeq 1.50$.

The magnetic susceptibility, plotted in Fig. 2, displays two peaks, in contrast to the single peak observed in the case of uncorrelated disorder (see the inset of Fig. 2). These two peaks appear at temperatures similar to those for which an abrupt variation of magnetization was observed. The magnetic susceptibility diverges algebraically with the lattice size for all temperatures in the region between the two peaks (note the use of a logarithmic scale for the y-axis on the figure). The critical exponent associated to this divergence will be discussed in the next section. We are therefore in presence of a Griffiths phase, like in the McCoy-Wu model. As mentioned in the introduction, the occurrence of such a Griffiths phase in the McCoy-Wu model was explained by the existence of exponentially rare macroscopic regions that can order independently of the rest of the system. The susceptibility of each disorder configuration is plotted on Fig. 3 versus the polarization density $p = \langle \sigma_i \tau_i \rangle$ of the auxiliary Ashkin-Teller model. By construction (9), p depends linearly on the concentration of strong couplings J_2. The value $p = -1$ corresponds to the configuration with only weak couplings J_1 while all couplings are strong when $p = +1$. As can be observed on Fig. 3, the largest susceptibility is observed for disorder configurations with different polarizations as the temperature is increased. In the paramagnetic phase (left of Fig. 3), the largest susceptibility is due to configurations with a high concentration of strong couplings. To understand this behavior, consider the two configurations with identical couplings, either J_1 or J_2. The system is expected to behave like a pure Potts model. Therefore, at large temperature $\beta J_1 < \beta J_2 < \beta_c$, a lattice of strong couplings J_2 is closer to the transition point than a configuration with mainly weak couplings J_1. Analogously, in the ferromagnetic phase (right of Fig. 3), the average susceptibility is dominated by disorder configurations with small concentrations of strong couplings. In the Griffiths phase (center of Fig. 3), the main contribution comes from disorder configurations with a slightly negative polarization, i.e. a number of strong couplings slightly below the number of weak ones. In such configurations, different clusters of weak or strong couplings are typically observed. The average magnetization is around 0.4, which means that the largest cluster of strong couplings occupies at most 40% of the sites. There is therefore plenty of space left for other clusters, possibly macroscopic too. Note that the width of the bunch of points in Fig. 3 increases in the Griffiths phase: at fixed polarization, some disorder configurations lead to susceptibilities ~ 60 times larger than others. In the case of uncorrelated disorder, we did not find any temperature, among those studied, for which the plot of susceptibilities versus polarization looks like Fig. 3 in the Griffiths phase.

In the case of uncorrelated disorder, it is well known that sample-to-sample fluctuations increase drastically with the lattice size at the critical point. One consequence is the lack of self-averaging of thermodynamic quantities. Averages are then dominated by rare, rather than typical, events. In the (uncorrelated) random Potts model, self-averaging is broken only at the critical point. Below and above, self-averaging is restored in the thermodynamic limit. In the correlated case, magnetization is a non self-averaging quantity in the whole Griffiths phase. Following Wiseman and Domany [36], the lack of self-averaging of magnetization is measured by comparing the variance with the average:

$$R_m = \frac{\overline{\langle m \rangle^2} - \overline{\langle m \rangle}^2}{\overline{\langle m \rangle}^2}. \tag{11}$$

This ratio is expected to go to a non-vanishing limit in the thermodynamic limit when self-averaging is not satisfied. As can be seen on Fig. 4, this is the case in the Griffiths phase. The value taken by R_m in the thermodynamic limit is expected to be universal [37]. While no dependence on the strength of disorder is observed, R_m is however not constant in the Griffiths phase but depends on the temperature. This implies that the critical behavior in the Griffiths phase is not described by a single universality class. We will come back to that point in next section. In the case of uncorrelated case, presented in the inset of Fig. 4, the ratio R_m vanishes at all temperatures except the critical one.

Like the magnetic susceptibility, the specific heat displays two peaks (Fig. 5). However, it depends only weakly on the lattice size. At the peaks, the data are compatible for all lattice sizes. In between, a small increase of the specific heat with the lattice size is observed. Note that the scale of the y-axis is only linear and not logarithmic, so the evolution with the lattice size is extremely slow. When plotted versus the polarization, the specific heat of the different disorder configurations presents a much more weakly bended shape than the magnetic susceptibility. The largest and smallest specific heats differ at most by a factor ~ 2. The computation of the ratio

$$R_e = \frac{\overline{\langle e \rangle^2} - \overline{\langle e \rangle}^2}{\overline{\langle e \rangle}^2} \tag{12}$$

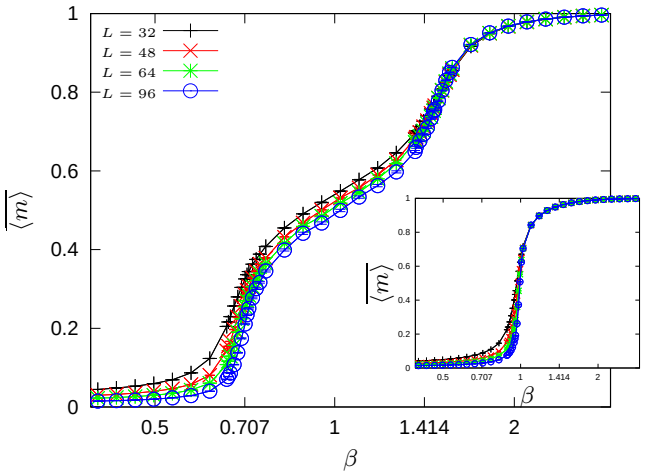

FIG. 1. Average magnetization of the Ising model ($q = 2$), with a disorder strength $r = 3$ and a correlation exponent $a = 0.4$ ($y = 0.75$), versus the inverse temperature $\beta = 1/k_BT$. The different curves correspond to different lattice sizes ($L = 32, 48, 64$ and 96). In the inset, the magnetization curve in the case of uncorrelated disorder is plotted.

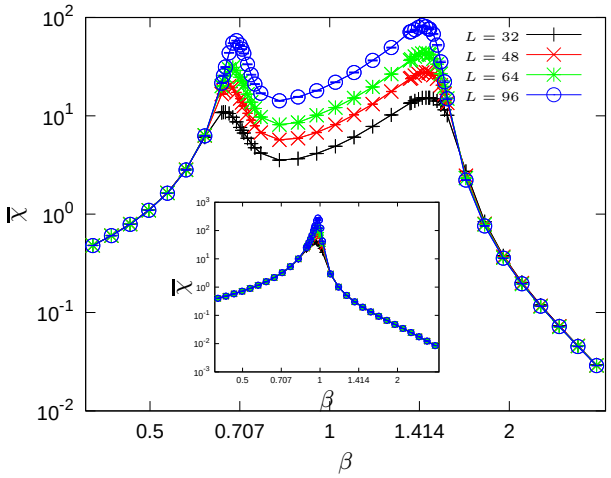

FIG. 2. Average susceptibility of the Ising model ($q = 2$), with a disorder strength $r = 3$ and a correlation exponent $a = 0.4$ ($y = 0.75$), versus the inverse temperature $\beta = 1/k_BT$. The different curves correspond to different lattice sizes ($L = 32, 48, 64$ and 96). In the inset, the average susceptibility in the case of uncorrelated disorder is plotted.

reveals that energy is a self-averaging quantity at all temperatures, including the critical temperature. This is also the case for uncorrelated disorder. To conclude, no evidence of Griffiths phase is found with thermal quantities, in contrast to the magnetic sector.

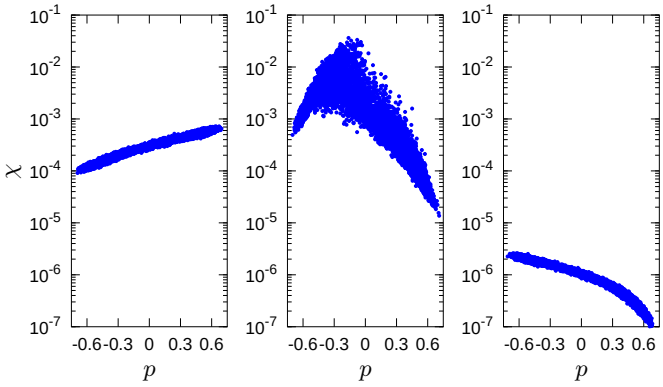

FIG. 3. Susceptibility χ of the Ising model with correlated disorder ($a = 0.4$, $r = 3$) versus the polarization density p of the disorder realization for $\beta \simeq 0.535$ (left), 1.022 (center) and 2.801 (right). Each point corresponds to a different disorder realization. The lattice size is $L = 96$.

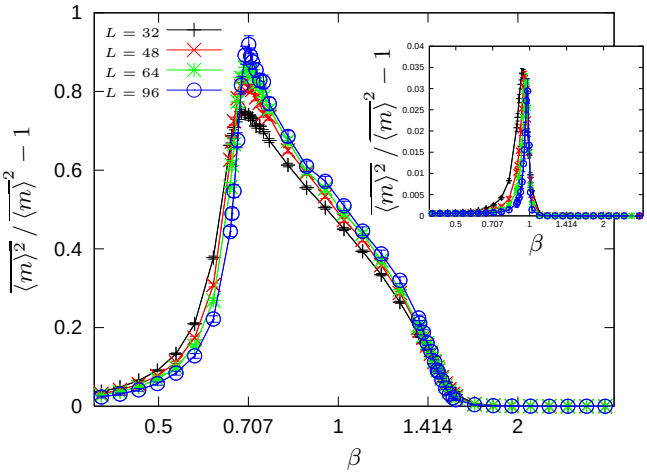

FIG. 4. Self-averaging ratio R_m of magnetization of the Ising model ($q = 2$), with a disorder strength $r = 3$ and a correlation exponent $a = 0.4$ ($y = 0.75$), versus the inverse temperature $\beta = 1/k_BT$. In the inset, ratio in the case of uncorrelated disorder.

B. $q = 8$ Potts model

The 8-state Potts model with correlated disorder displays a behavior very similar to that of the Ising model presented above. Like in the case of uncorrelated disorder, the fact that the pure system undergoes a first-order phase transition does not lead to any significant difference. The magnetization curve displays two abrupt variations (Fig. 6). The location of these fast variations coincides with the two peaks of the magnetic susceptibility (Fig. 7). For the 8-state Potts model, a stronger disorder $r = 7.5$ was considered, which means that $J_1 \simeq 0.3855$ and $J_2 \simeq 2.891$. In contrast to the Ising case, the first temperature scale $\beta = \frac{1}{k_BT} = \frac{1}{J_2} \simeq 0.3459$

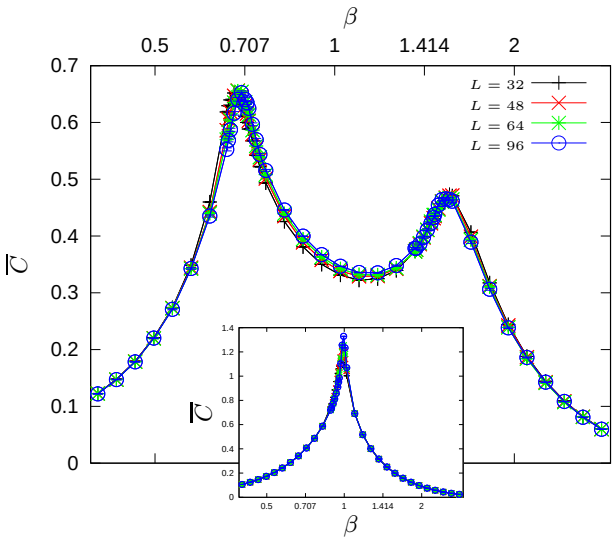

FIG. 5. Average specific heat of the Ising model ($q = 2$), with a disorder strength $r = 3$ and a correlation exponent $a = 0.4$ ($y = 0.75$), versus the inverse temperature $\beta = 1/k_BT$. The different curves correspond to different lattice sizes ($L = 32, 48, 64$ and 96). In the inset, the specific heat in the case of uncorrelated disorder is plotted.

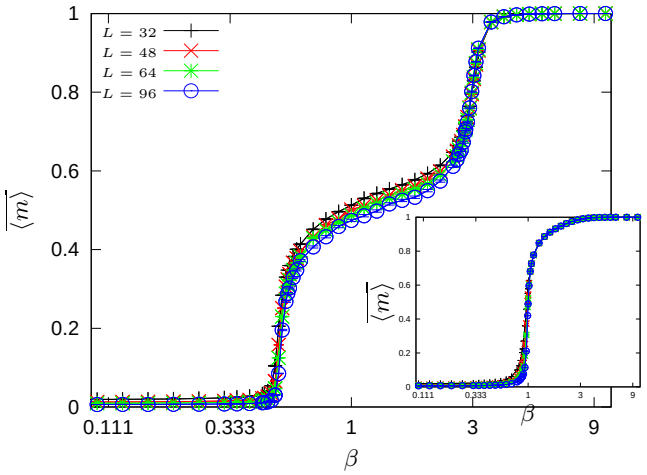

FIG. 6. Average magnetization of the 8-state Potts model, with a disorder strength $r = 7.5$ and a correlation exponent $a = 0.4$ ($y = 0.75$), versus the inverse temperature $\beta = 1/k_BT$. In the inset, magnetization curve in the case of uncorrelated disorder.

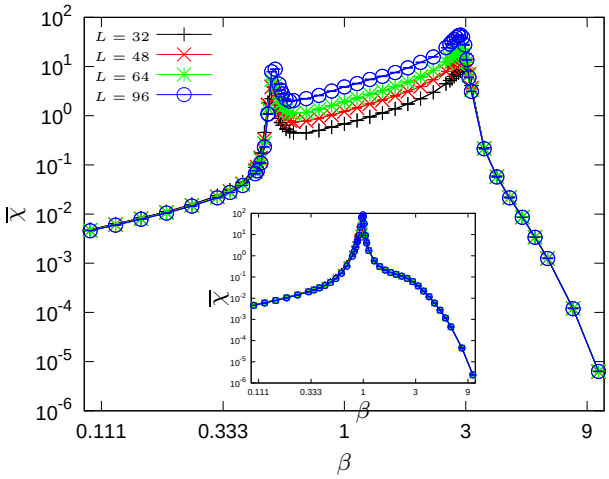

FIG. 7. Average susceptibility of the 8-state Potts model, with a disorder strength $r = 7.5$ and a correlation exponent $a = 0.4$ ($y = 0.75$), versus the inverse temperature $\beta = 1/k_BT$. In the inset, susceptibility in the case of uncorrelated disorder.

is significantly smaller than the location of the first peak (around 0.50). The second temperature scale $\frac{1}{J_1} \simeq 2.594$ is smaller than the location of the second peak. When plotted versus the polarization of the auxiliary Ashkin-Teller model, the susceptibilities of the different disorder configurations are very similar to those of Fig. 3. In the Griffiths phase, the largest susceptibilities are again observed at a small negative polarization ($\simeq -0.05$,) i.e. for disorder configurations with a slightly smaller number of strong couplings than weak ones. The main difference with the Ising model is a much larger spreading of the bunch of points. The ratio between the largest and the smallest susceptibilities at fixed polarization is ~ 330. The ratio Eq. 11 is plotted on Fig. 8 in the case of the 8-state Potts model. Like in the Ising case, magnetization is not self-averaging in the Griffiths phase.

The specific heat does not display such properties. Even though two peaks can be observed (Fig. 9), the specific heat is essentially size-independent, even at and between the two peaks. The ratio Eq. 12 vanishes at all temperatures which implies that energy is a self-averaging quantity.

IV. CRITICAL BEHAVIOR IN THE GRIFFITHS PHASE

In Ref. [29], the critical exponents have been estimated at the self-dual point $\beta_c = 1$ of the 8-state Potts model with correlated disorder. In the following, the study is extended to the $q = 2, 4$ and 16-state Potts models, and to several other temperatures in the Griffiths phase. Numerical evidence of the stability of the critical exponents against a variation of the strength of disorder is provided.

Monte Carlo simulations were performed for lattice sizes $L = 16$, 24, 32, 48, 64, 96, 128, 192, and 256. The thermodynamic quantities were averaged over a number of disorder configurations proportional to $1/L^2$. For the largest lattice size ($L = 256$), 10240 disorder configurations were generated while for $L = 64$ for example, this number is raised up to 163840. For each disorder configuration, 5000 Monte Carlo steps are performed. The critical exponents β/ν, γ/ν and ν are determined by Finite-

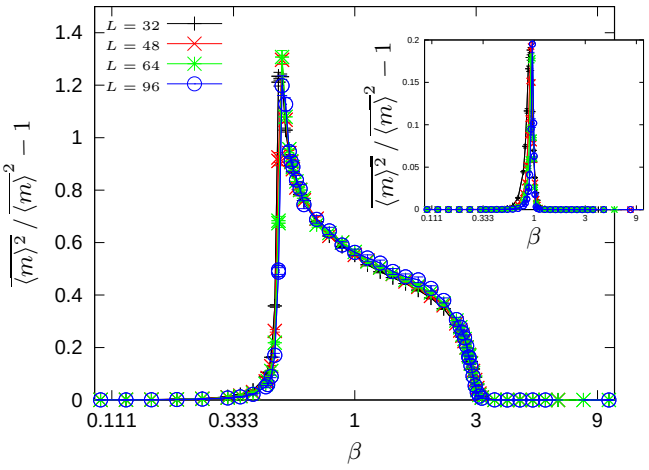

FIG. 8. Self-averaging ratio R_m of magnetization of the 8-state Potts model, with a disorder strength $r = 7.5$ and a correlation exponent $a = 0.4$ ($y = 0.75$), versus the inverse temperature $\beta = 1/k_BT$. In the inset, ratio in the case of uncorrelated disorder.

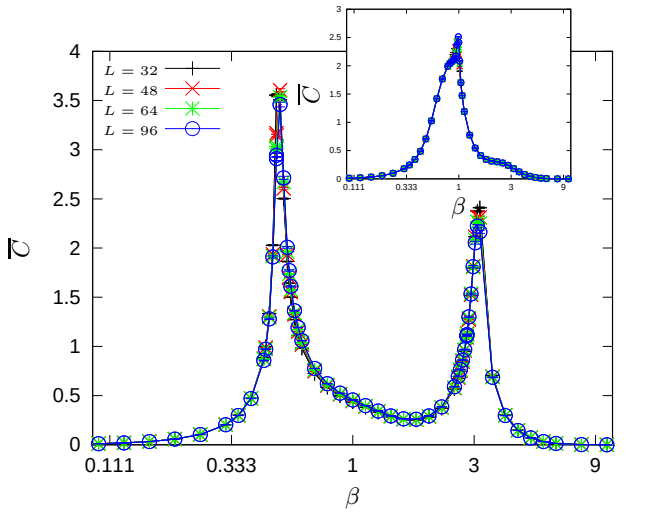

FIG. 9. Average specific heat of the 8-state Potts model, with a disorder strength $r = 7.5$ and a correlation exponent $a = 0.4$ ($y = 0.75$), versus the inverse temperature $\beta = 1/k_BT$. In the inset, the specific heat in the case of uncorrelated disorder.

Size Scaling of the average quantities:

$$\overline{\langle m^n\rangle}^{1/n} \sim L^{-\beta/\nu},$$
$$\overline{\chi} = \beta L^d \left[\overline{\langle m^2\rangle} - \overline{\langle m\rangle^2}\right] \sim L^{\gamma/\nu},$$
$$-\frac{d \ln \overline{\langle m\rangle}}{d\beta} = L^d \frac{\overline{\langle me\rangle} - \overline{\langle m\rangle\langle e\rangle}}{\overline{\langle m\rangle}} \sim L^{1/\nu} \qquad (13)$$

where the moments of order $n = 1, 2, 3$ and 4 of the magnetization are considered. To take into account the possibility of scaling corrections, relatively strong for the average susceptibility, power-law fits are successively performed in the windows $[L_{\min}, 256]$ where the smallest lattice size $L_{\min.}$ is iteratively increased. The different fits lead to $L_{\min.}$-dependent effective critical exponents. Because of scaling corrections, these exponents do not reach a plateau at large $L_{\min.}$ but rather vary continuously with $L_{\min.}$. An extrapolation of these effective exponents in the limit $1/L_{\min.} \to 0$ is performed. For most of the observables, it is sufficient to consider an extrapolation with a polynomial of degree 1 in $1/L_{\min.}$.

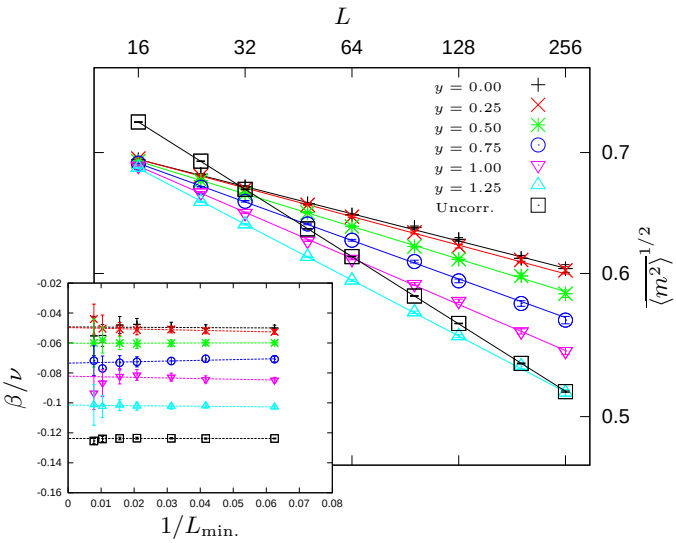

FIG. 10. Finite-Size Scaling of the second moment $\overline{\langle m^2\rangle}^{1/2}$ of the magnetization of the Ising model ($q = 2$) with a disorder strength $r = 3$ at the self-dual point $\beta_c = 1$. The different curves correspond to different disorder correlation exponents, referred to by the parameter y of the auxiliary Ashkin-Teller model. The curve with the legend Uncorr. corresponds to the Ising model with uncorrelated disorder. In the inset, effective exponents obtained by fitting the data in the window $[L_{\min}; 256]$ versus $1/L_{\min}$. The straight line is a linear fit of these exponents.

Among the various moments of magnetization that were considered, the second one displays the smallest scaling corrections. As can be seen on Fig. 10 in the case of the Ising model, the effective exponent β/ν does not vary much with the lowest lattice size $L_{\min.}$ entering into the power-law fit of $\overline{\langle m^2\rangle}^{1/2}$. For the average magnetization and the moments of order 3 and 4, a slow linear variation of these exponents is observed. A linear extrapolation leads in the limit $L_{\min.} \to 0$ to exponents compatible with those obtained from the second moment. The different exponents at the self-dual point $\beta_c = 1$ are collected in Table I. The exponents do not show any significant dependence on the strength of disorder r. As already observed in the case of uncorrelated disorder, the amplitude of the scaling corrections depends on r. More interesting is the fact that the exponents β/ν do not depend on the number of states q of the Potts model. As mentioned in the introduction, such a behavior is also observed in the generalization of the McCoy-Wu model to Potts spins. However, the estimates of β/ν are remarkably different from the

TABLE I. Critical exponent β/ν extrapolated from the Finite-Size Scaling of the second moment $\overline{\langle m^2 \rangle}^{1/2}$ of magnetization at the self-dual point $\beta_c = 1$. The estimates for uncorrelated disorder can be compared with the exact value 1/8 ($q = 2$) and the transfer matrix estimates 0.1419(1) ($q = 4$), 0.1514(2) ($q = 8$) from Ref. [38].

y	0	0.25	0.5	0.75	1	1.25	Uncorr. Dis.
$q = 2$, $r = 2$	0.046(6)	0.051(7)	0.059(6)	0.069(6)	0.078(5)	0.102(7)	0.1250(7)
$q = 2$, $r = 3$	0.049(7)	0.050(5)	0.060(4)	0.073(5)	0.082(6)	0.102(4)	0.1238(11)
$q = 4$, $r = 4$	0.052(6)	0.049(7)	0.064(6)	0.071(6)	0.088(7)	0.102(5)	0.139(2)
$q = 8$, $r = 6$	0.053(6)	0.057(7)	0.066(7)	0.075(6)	0.092(6)	0.104(5)	0.150(2)
$q = 8$, $r = 7.5$	0.052(6)	0.059(5)	0.067(6)	0.076(6)	0.087(5)	0.104(4)	0.150(2)
$q = 8$, $r = 9$	0.052(5)	0.056(7)	0.068(7)	0.074(6)	0.088(5)	0.108(8)	0.149(3)
$q = 16$, $r = 10$	0.052(5)	0.056(6)	0.066(7)	0.072(7)	0.089(5)	0.108(5)	0.159(3)

exact value $\beta/\nu = (3 - \sqrt{5})/4$ at the McCoy-Wu-Fisher fixed point. Furthermore, it can be observed in Table I that the exponent β/ν increases when the disorder correlations decay faster, i.e. when y, and therefore a, increases. β/ν remains always smaller than in the case of uncorrelated disorder. Such a behavior was also observed for the McCoy-Wu model with correlated disorder in the longitudinal direction [21]. However, the magnetic scaling dimension was shown to be $\beta/\nu \simeq a/2$ in this model while this exponent is closer to $a/5$ in the Potts model with correlated disorder. The dependence of β/ν on a also contradicts Weinrib and Halperin calculation for which $\beta/\nu = \mathcal{O}(\epsilon^2)$ in 2D. Therefore, the Potts model with the correlated disorder considered in this paper belongs to a distinct universality class.

The independence of the exponents with the number of states q contrasts with the case of the Potts model with uncorrelated disorder for which an increase of β/ν with q was shown. A very small dependence of β/ν on q, compatible with error bars, cannot be completly excluded. Note that in the case of the McCoy-Wu model with correlated disorder, the exponent β/ν is a continuous function of the correlation exponent a, even at $a = 1$ corresponding in this case to uncorrelated disorder [21]. If the same occurs for the isotropic Potts model with correlated disorder, then one should expect a dependence on q for exponents $a < 2$ because such a dependence exists for uncorrelated disorder, i.e. for $a \geq 2$. This hypothesis could be tested with values of a close to 2. Unfortunately, the use of the Ashkin-Teller as an auxiliary model to generate the disorder configurations does not allow to go beyond $a = 3/4$ ($y = 4/3$) and therefore closer to the point $a = 2$. Another possible scenario is that the RG flow for the Potts model with correlated disorder is similar to the case studied by Weinrib and Halperin. For small values $a < d = 2$, the independence of the exponent β/ν on q could be explained by a critical behavior which is controlled by the same correlated-disorder fixed point for all Potts models. Above $a = d = 2$, the latter becomes unstable and the critical behavior is then governed by the short-range or uncorrelated fixed point

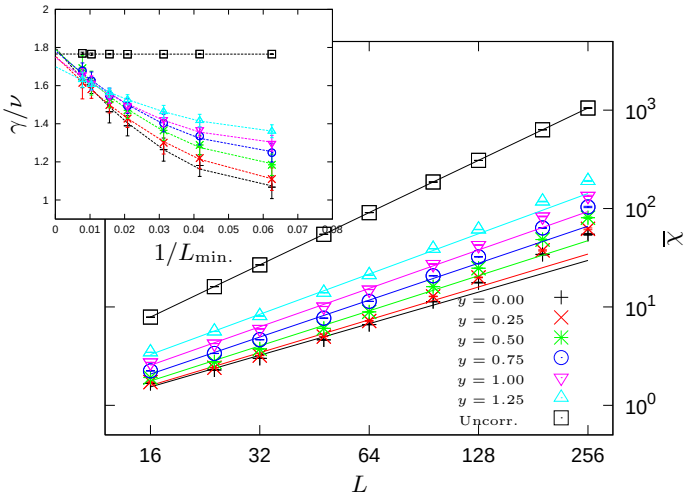

FIG. 11. Finite-Size Scaling of the average susceptibility $\overline{\chi}$ of the Ising model ($q = 2$) with a disorder strength $r = 3$ at the critical point $\beta_c = 1$. The different curves correspond to different disorder correlation exponents, referred to by the parameter y of the auxiliary Ashkin-Teller model. The curve with the legend Uncorr. corresponds to the Ising model with uncorrelated disorder. In the inset, effective exponents obtained by fitting the data in the window $[L_{\min}; 256]$ versus $1/L_{\min}$. The solid line is a parabolic fit of these exponents.

where the exponents are known to be q-dependent.

In the Griffiths phase, the dependence of the exponents on the temperature was tested for the Ising and 8-state Potts models. Estimates of β/ν are given in Table II. In the Ising case, only one temperature was tested and the corresponding estimates of the exponent β/ν are incompatible with the value measured at the self-dual point for all parameters $y \geq 0.5$. In the Potts case, the Griffiths phase is larger and three well separated temperatures were considered. The exponent β/ν clearly increases with the temperature for all values of y. The Griffiths phase is therefore not described by a unique fixed point. This result corroborates the existence of a non-constant asymptotic value of R_m, supposed to be universal, in the Griffiths phase.

TABLE II. Critical exponent β/ν extrapolated from the Finite-Size Scaling of the second moment $\overline{\langle m^2\rangle}^{1/2}$ of magnetization at different temperatures in the Griffiths phase.

y	0	0.25	0.5	0.75	1	1.25
$q=2$, $\beta=1$	0.049(7)	0.050(5)	0.060(4)	0.073(5)	0.082(6)	0.102(4)
$q=2$, $\beta=1.2$	0.040(6)	0.044(5)	0.048(4)	0.050(4)	0.063(4)	0.043(7)
$q=8$, $\beta=0.75$	0.057(7)	0.062(5)	0.073(5)	0.092(6)	0.110(7)	0.138(6)
$q=8$, $\beta=1$	0.052(6)	0.059(5)	0.067(6)	0.076(6)	0.087(5)	0.104(4)
$q=8$, $\beta=1.5$	0.050(5)	0.052(5)	0.055(5)	0.64(7)	0.073(7)	0.082(5)
$q=8$, $\beta=2$	0.041(6)	0.045(5)	0.052(6)	0.056(6)	0.061(4)	0.052(4)

TABLE III. Critical exponent γ/ν extrapolated from the Finite-Size Scaling of the average susceptibility $\overline{\chi}$ at the self-dual point $\beta_c = 1$. A polynomial of degree 2 was used for the extrapolation. The estimates for uncorrelated disorder can be compared with the exact value 7/4 ($q=2$) and the transfer matrix estimates 1.7162(2) ($q=4$), 1.6972(4) ($q=8$) from Ref. [38] assuming that hyperscaling holds.

y	0	0.25	0.5	0.75	1	1.25	Uncorr. Dis.
$q=2$, $r=2$	1.66(7)	1.73(9)	1.69(12)	1.66(7)	1.64(6)	1.64(7)	1.759(6)
$q=2$, $r=3$	1.80(7)	1.76(8)	1.79(10)	1.78(7)	1.75(6)	1.70(4)	1.766(8)
$q=4$, $r=4$	1.84(9)	1.80(7)	1.80(5)	1.74(5)	1.81(5)	1.77(7)	1.717(13)
$q=8$, $r=6$	1.77(12)	1.77(7)	1.79(7)	1.80(8)	1.77(6)	1.75(7)	1.68(2)
$q=8$, $r=7.5$	1.77(7)	1.75(8)	1.78(6)	1.78(8)	1.75(7)	1.74(5)	1.70(3)
$q=8$, $r=9$	1.78(9)	1.84(11)	1.80(8)	1.77(6)	1.72(6)	1.74(6)	1.71(2)
$q=16$, $r=10$	1.78(10)	1.80(12)	1.79(9)	1.78(10)	1.72(6)	1.74(5)	1.75(3)

The estimation of the exponent γ/ν from the Finite-Size Scaling of the magnetic susceptibility is much more difficult. Much stronger scaling corrections are present, especially for small values of y. These corrections manifest themselves on Fig. 11 as a gap between the numerical data at large lattice sizes and the power-law fit plotted as a continuous line. The effective exponents indeed start with values in the range $[1.1; 1.3]$ and then increase as more and more small lattice sizes are removed from the fit (see inset of Fig. 11). When only lattice sizes $L \geq 128$ are taken into account in the fit, the effective exponents take values around $1.6 - 1.7$, the value reported in Ref. [29]. On the figure, the effective exponents increase with the parameter y and tend towards a value close to the exponent of the uncorrelated disorder. Because of the curvature displayed by the effective exponents when plotted versus $1/L_{\text{min.}}$, a simple linear extrapolation, like in the case of magnetization, does not take into account reliably the scaling corrections. It turns out that the exponents fall nicely on the parabolic fit represented on the figure. However, the use of a polynomial of degree 2 reduces the number of degrees of freedom of the fit, and thus increases the error bar and lowers the stability of the extrapolated exponents. The latter are given in Tables III and IV. No significant dependence on the number of states q, the strength of disorder r, nor the temperature in the Griffiths phase can be noticed. While the estimates of γ/ν are compatible between each other, half of them are not compatible with the hyperscaling relation

$$\frac{\gamma}{\nu} = d - 2\frac{\beta}{\nu}. \tag{14}$$

On Fig. 12, the ratio $\overline{\chi}\ /\ L^d\overline{\langle m\rangle}^2$ is plotted versus the lattice size in the case of the Ising model. This quantity is expected to scale as L^0 when the hyperscaling relation Eq. 14 holds. A power-law behavior is indeed observed at large lattice sizes, though with a smaller exponent than at small lattice sizes. A fit over the three largest lattice sizes leads to negative exponents, compatible within error bars with zero, i.e. the hyperscaling relation, in only 20% of all cases considered. This statement is also true at different temperatures in the Griffiths phase. Of course, we cannot completely exclude the possibility of a restoration of the hyperscaling relation at larger lattice sizes. In the case of uncorrelated disorder, the data are in much better agreement with the hyperscaling relation.

As commented in the first section, the specific heat does not seem to display any divergence in the Griffiths phase. Even with larger lattice sizes, up to $L = 256$, it is not possible to isolate any singular part from a regular background. It means that the specific heat exponent α/ν is therefore smaller or equal to zero. The Finite-Size Scaling of the derivative of the logarithm of the average magnetization with respect to temperature gives access to the exponent ν [39]. In contrast to the magnetic susceptibility, a linear fit of the $L_{\text{min.}}$-dependent effective exponents is sufficient to properly take into account the

TABLE IV. Critical exponent γ/ν extrapolated from the Finite-Size Scaling of the average susceptibility $\overline{\chi}$ at different temperatures in the Griffiths phase. A polynomial of degree 2 was used for the extrapolation.

y	0	0.25	0.5	0.75	1	1.25
$q=2,\ \beta=1$	1.80(7)	1.76(8)	1.79(10)	1.78(7)	1.75(6)	1.70(4)
$q=2,\ \beta=1.2$	1.64(5)	1.70(8)	1.73(8)	1.71(5)	1.76(4)	1.69(4)
$q=8,\ \beta=0.75$	1.80(11)	1.86(8)	1.78(9)	1.68(6)	1.71(7)	1.68(4)
$q=8,\ \beta=1$	1.77(7)	1.75(8)	1.78(6)	1.78(8)	1.75(7)	1.74(5)
$q=8,\ \beta=1.5$	1.80(10)	1.70(8)	1.72(6)	1.77(6)	1.78(8)	1.78(5)
$q=8,\ \beta=2$	1.68(8)	1.74(9)	1.78(8)	1.74(6)	1.71(8)	1.78(4)

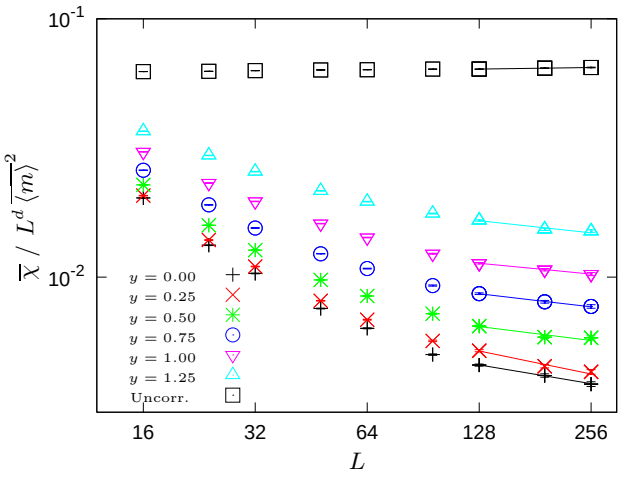

FIG. 12. $\overline{\chi}\ /\ L^d\overline{\langle m\rangle}^2$ versus the lattice size L for the Ising model ($q = 2$) with a disorder strength $r = 3$ at the self-dual point $\beta_c = 1$. According to the hyperscaling relation, this ratio should scale as L^0. The straight line is a power-law fit over the three last lattice sizes. The slopes, as given by the fit, are $-0.24(5)$, -0.38(10), $-0.3(2)$, $-0.30(5)$, $-0.31(6)$, $-0.18(3)$ for $y = 0.00$, 0.25, 0.50, 0.75, 1.00 and 1.25. For uncorrelated disorder, this value is 0.012(10).

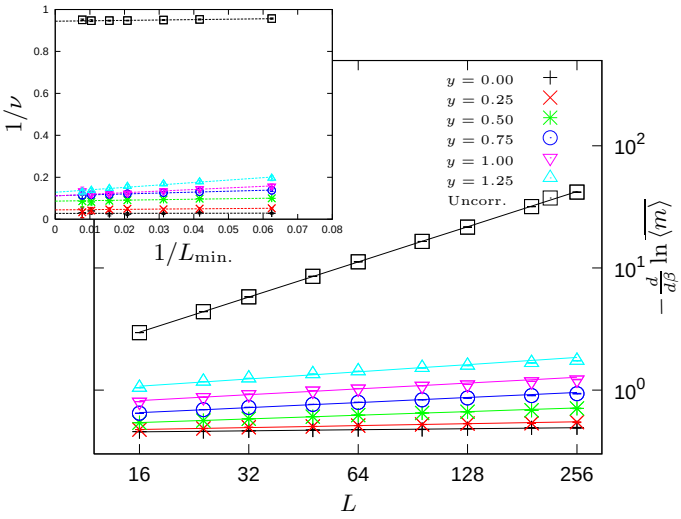

FIG. 13. Finite-Size Scaling of $-\frac{d}{d\beta}\ln\overline{\langle m\rangle}$ for the Ising model ($q = 2$) with a disorder strength $r = 3$ at the critical point $\beta_c = 1$. The different curves correspond to different disorder correlation exponents, referred to by the parameter y of the auxiliary Ashkin-Teller model. The curve with the legend Uncorr. corresponds to the Ising model with uncorrelated disorder. In the inset, effective exponents $1/\nu$ obtained by fitting the data in the window $[L_{\min}; 256]$ versus $1/L_{\min}$. The straight line is a linear fit of these exponents.

scaling corrections (see Fig. 13). The extrapolated exponents are given in Tables V and VI. In a few cases, the extrapolation procedure appears to be unstable: several spurious values can be seen in the tables (for example for $q = 8, r = 7.5, y = 0$ or $q = 2, \beta = 1.2$). From the rest of the data, the same trends as for magnetization are observed: the exponents do not significantly vary with the strength of disorder r, nor the number of states q. However, in contrast to magnetization, a dependence on temperature is not clearly seen. More accurate values would be necessary. Note that the exponent ν takes values incompatible with the Weinrib-Halperin prediction $\nu = 2/a$ for the $O(n)$ model. For comparison, the latter would give $1/\nu = 0.125$, 0.143, 0.167, 0.2, 0.25 and 0.333 for the values of a that were considered. Finally, note that the hyperscaling relation $\frac{\alpha}{\nu} = \frac{2}{\nu} - d$ leads, with the estimates of ν reported in Tables V and VI, to negative specific heat exponents $\frac{\alpha}{\nu} < -1.7$. Because of the regular contribution to the specific heat, this prediction cannot be tested.

V. DISORDER FLUCTUATIONS AND HYPERSCALING VIOLATION

As pointed out in the previous section, the average susceptibility diverges with an exponent γ/ν which is close, but not perfectly compatible, with the hyperscaling relation and the magnetization exponent β/ν. As pointed out in Ref [29], this violation of hyperscaling is the result of large disorder fluctuations, as in the 3D random-field Ising model [40] (RFIM). We briefly describe in the following the arguments of [29]. The average magnetic susceptibility, as given by the derivative of the average magnetization with respect to an external magnetic field,

TABLE V. Critical exponent $1/\nu$ extrapolated from the Finite-Size Scaling of the quantity $-\frac{d}{d\beta}\ln\overline{\langle m\rangle}$ at the self-dual point $\beta_c = 1$. For uncorrelated disorder, estimates of ν slightly above 1, but usually compatible, were reported in the literature [2, 10]. In the case $q = 2$, $\nu = 1$ (with logarithmic corrections) since uncorrelated disorder is marginally irrelevant.

y	0	0.25	0.5	0.75	1	1.25	Uncorr. Dis.
$q = 2$, $r = 2$	0.041(10)	0.065(12)	0.099(13)	0.116(13)	0.11(2)	0.14(2)	0.969(4)
$q = 2$, $r = 3$	0.028(13)	0.044(11)	0.086(10)	0.112(9)	0.11(2)	0.13(2)	0.944(5)
$q = 4$, $r = 4$	0.033(12)	0.041(13)	0.082(12)	0.103(14)	0.113(14)	0.116(13)	0.985(7)
$q = 8$, $r = 6$	0.026(11)	0.05(2)	0.08(2)	0.101(11)	0.115(11)	0.113(11)	0.965(11)
$q = 8$, $r = 7.5$	0.25(10)	0.047(12)	0.083(9)	0.107(10)	0.111(9)	0.114(7)	0.976(9)
$q = 8$, $r = 9$	0.018(11)	0.041(12)	0.075(12)	0.097(11)	0.102(9)	0.109(12)	0.972(7)
$q = 16$, $r = 10$	0.022(10)	0.04(2)	0.069(10)	0.083(14)	0.101(10)	0.113(9)	1.02(3)

TABLE VI. Critical exponent $1/\nu$ estimated from the Finite-Size Scaling of the quantity $-\frac{d}{d\beta}\ln\overline{\langle m\rangle}$ at different temperatures in the Griffiths phase.

y	0	0.25	0.5	0.75	1	1.25
$q = 2$, $\beta = 1$	0.028(13)	0.044(11)	0.086(10)	0.112(9)	0.11(2)	0.13(2)
$q = 2$, $\beta = 1.2$	−0.03(2)	0.00(2)	0.05(2)	0.059(12)	0.13(2)	0.31(2)
$q = 8$, $\beta = 0.75$	0.04(2)	0.06(2)	0.09(2)	0.11(2)	0.13(2)	0.187(11)
$q = 8$, $\beta = 1$	0.025(10)	0.047(12)	0.083(9)	0.107(10)	0.111(9)	0.114(7)
$q = 8$, $\beta = 1.5$	0.03(2)	0.04(2)	0.07(2)	0.103(14)	0.10(2)	0.146(13)
$q = 8$, $\beta = 2$	0.01(2)	0.03(2)	0.08(2)	0.079(13)	0.11(2)	0.336(13)

can be decomposed as

$$\begin{aligned}\overline{\chi} &= \beta L^d\big[\overline{\langle m^2\rangle} - \overline{\langle m^2\rangle}\big] \\ &= \underbrace{\beta L^d\big[\overline{\langle m^2\rangle} - \overline{\langle m\rangle}^2\big]}_{=\chi_1} - \underbrace{\beta L^d\big[\overline{\langle m\rangle^2} - \overline{\langle m\rangle}^2\big]}_{=\chi_2} \quad (15)\end{aligned}$$

The two terms, denoted χ_1 and χ_2, scale differently from the average susceptibility, i.e. their difference. The second term χ_2 is the numerator of the ratio R_m, defined by Eq. 11. Because the latter tends to a finite constant in the Griffiths phase (see Fig. 11), $\overline{\langle m\rangle^2} - \overline{\langle m\rangle}^2$ scales as $\overline{\langle m\rangle}^2$, i.e. as $L^{-2\beta/\nu}$. Therefore, including the L^d prefactor, the susceptibility χ_2 scales as $L^{d-2\beta/\nu}$, i.e. precisely as predicted by the hyperscaling relation Eq. 14. The numerical study of the Finite-Size Scaling of χ_1 reveals that it displays the same scaling behavior. As can be seen on Fig. 14 in the case of the Ising model and Fig. 15 for the 8-state Potts model, χ_1 is very different from the average susceptibility. Instead of two peaks separating a region of divergent susceptibility, a single broader peak is observed. Uncorrelated disorder leads to a thiner and thiner peak, like the average susceptibility. For all temperatures in the Griffiths phase, χ_1 diverges algebraically with an exponent that will be denoted $(\gamma/\nu)^*$ in the following. In the context of the 3D RFIM, $(\gamma/\nu)^* = 4 - \bar{\eta}$ [41]. The exponent $(\gamma/\nu)^*$ is estimated by following the same procedure as in the previous section. Effective exponents are first extracted by varying the fitting window. In contrast to the average magnetic susceptibility, χ_1 displays relatively weak scaling corrections so the effective exponents can safely be extrapolated with a linear fit. The extrapolated exponents $(\gamma/\nu)^*$ are presented in Tables VII and VIII. $(\gamma/\nu)^*$ depends on the disorder correlation exponent a but not on the number of states q, nor the strength of disorder r. The temperature dependence in the Griffiths phase is clearly seen for the largest values of y. As claimed above, the exponents are compatible with the hyperscaling relation and the estimates of β/ν for any Potts model and at any temperature in the Griffiths phase.

Not only χ_1 and χ_2 have the same scaling behavior but their dominant scaling terms also have the same amplitude A, i.e.

$$\chi_i = AL^{d-2\beta/\nu}\big(1 + B_i L^{-\omega_i} + \dots\big), \quad (i = 1, 2). \quad (16)$$

As a consequence, their difference behaves at large lattice sizes as

$$\overline{\chi} = \chi_1 - \chi_2 \sim AB_1 L^{d-2\beta/\nu-\omega_1} - AB_2 L^{d-2\beta/\nu-\omega_2} \quad (17)$$

i.e. with a scaling dimension $\gamma/\nu = d - 2\beta/\nu - \min(\omega_1, \omega_2)$. Our estimates of γ/ν, as given in Tables III and IV, and the analysis of the ratio $\overline{\chi}/L^d\overline{\langle m\rangle}^2$ (see for example Fig. 12) indicate that the deviation from the hyperscaling relation, i.e. $\min(\omega_1, \omega_2)$, is small (of order $0.1 - 0.3$). The only possibility for a restoration of hyperscaling at large lattice sizes is that the largest correction of either χ_1 or χ_2 diverge logarithmically, i.e. $\omega_1 = 0$ or $\omega_2 = 0$. In any other cases, one should expect a violation of hyperscaling. Note that the average susceptibility $\overline{\chi}$

TABLE VII. Critical exponent $(\gamma/\nu)^*$ extrapolated from the Finite-Size Scaling of the quantity χ_1 at the self-dual point $\beta_c = 1$.

y	0	0.25	0.5	0.75	1	1.25	Uncorr. Dis.
$q = 2$, $r = 2$	1.92(4)	1.91(4)	1.90(4)	1.88(4)	1.86(4)	1.83(4)	1.751(13)
$q = 2$, $r = 3$	1.91(3)	1.91(3)	1.89(3)	1.87(3)	1.85(3)	1.81(4)	1.75(2)
$q = 4$, $r = 4$	1.90(3)	1.89(3)	1.88(3)	1.86(3)	1.83(3)	1.79(3)	1.73(2)
$q = 8$, $r = 6$	1.90(2)	1.89(2)	1.87(2)	1.86(2)	1.82(3)	1.78(2)	1.72(4)
$q = 8$, $r = 7.5$	1.90(2)	1.90(2)	1.88(2)	1.85(2)	1.82(3)	1.79(3)	1.73(4)
$q = 8$, $r = 9$	1.91(2)	1.89(2)	1.88(2)	1.85(2)	1.83(3)	1.79(3)	1.75(4)
$q = 16$, $r = 10$	1.90(2)	1.89(2)	1.88(2)	1.86(2)	1.83(2)	1.78(3)	1.74(4)

TABLE VIII. Critical exponent $(\gamma/\nu)^*$ extrapolated from the Finite-Size Scaling of the quantity χ_1 at different temperatures in the Griffiths phase.

y	0	0.25	0.5	0.75	1	1.25
$q = 2$, $\beta = 1$	1.91(3)	1.91(3)	1.89(3)	1.87(3)	1.85(3)	1.81(4)
$q = 2$, $\beta = 1.2$	1.96(3)	1.95(4)	1.93(4)	1.92(4)	1.92(4)	1.79(6)
$q = 8$, $\beta = 0.75$	1.88(2)	1.87(2)	1.85(2)	1.82(2)	1.77(2)	1.72(2)
$q = 8$, $\beta = 1$	1.90(2)	1.90(2)	1.88(2)	1.85(2)	1.82(3)	1.79(3)
$q = 8$, $\beta = 1.5$	1.92(3)	1.92(3)	1.90(2)	1.89(2)	1.87(3)	1.84(3)
$q = 8$, $\beta = 2$	1.94(3)	1.94(3)	1.92(3)	1.91(3)	1.90(3)	1.78(5)

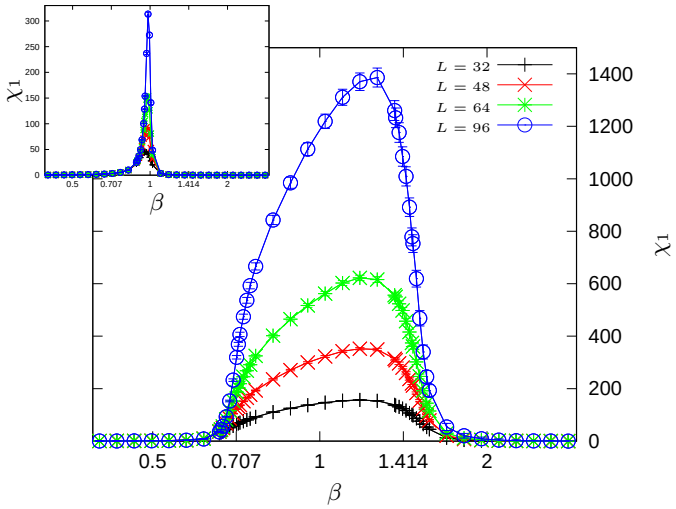

FIG. 14. Disorder fluctuations of magnetization χ_1 of the Ising model ($q = 2$), with a disorder strength $r = 3$ and a correlation exponent $a = 0.4$ ($y = 0.75$), versus the inverse temperature $\beta = 1/k_BT$. In the inset, disorder fluctuations in the case of uncorrelated disorder.

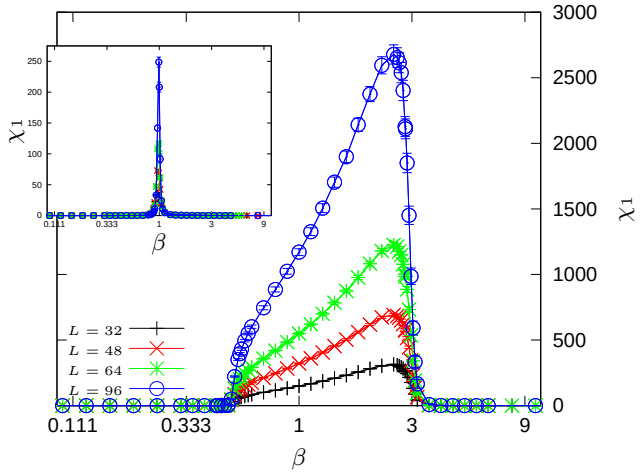

FIG. 15. Disorder fluctuations of magnetization χ_1 of the 8-state Potts model, with a disorder strength $r = 7.5$ and a correlation exponent $a = 0.4$ ($y = 0.75$), versus the inverse temperature $\beta = 1/k_BT$. In the inset, disorder fluctuations in the case of uncorrelated disorder.

is two to three orders of magnitude smaller than both χ_1 and χ_2, which means that $B_i \simeq 10^{-2}$. This is in agreement with the observation that χ_1 and χ_2 only display weak scaling corrections. To check that both χ_1 and χ_2 have the same dominant amplitude A, their ratio was analyzed. Two particular cases are presented on Fig. 16. On the left, the ratio χ_1/χ_2 for the Ising model goes to the expected limit 1 for all parameters y considered while for uncorrelated disorder, a very different limit is observed. On the right, this ratio is plotted in the case of the 8-state Potts at several temperatures in the Griffiths phase. Again, the data goes to the limit 1. The same analysis, reproduced for all numbers of states q, strength of disorder r, or temperatures in the Griffiths phase, leads to the same conclusion. In all cases, the leading amplitudes of χ_1 and χ_2 are shown to be identical. Consequently, the dominant contributions of χ_1 and

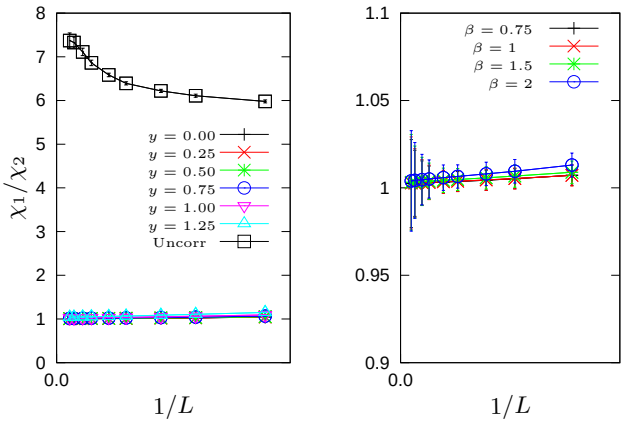

FIG. 16. Ratio χ_1/χ_2 versus the inverse $1/L$ of the lattice size for various parameters y in the case of the Ising model ($r = 3$) on the left and for several temperatures in the Griffiths phase of the 8-state Potts ($y = 0.75$ and $r = 7.5$) on the right.

χ_2 cancel out and the hyperscaling relation is broken in the entire Griffiths phase. In the case of uncorrelated disorder, the ratio goes to a value very different from 1 (see inset of Fig. 16). Therefore, the dominant contributions of χ_1 and χ_2 do not cancel out in this case and the hyperscaling relation is not broken.

The same analysis can be performed in the energy sector. However, as already mentioned, it is not possible to decide whether the hyperscaling relation $\frac{\alpha}{\nu} = \frac{2}{\nu} - d$ is broken or not because the specific heat does not diverge and therefore its singular part cannot be separated from the regular background. Nevertheless, one can check that the same mechanism is present, which implies that hyperscaling is broken unless the first correction is only logarithmic. The average specific heat is decomposed as

$$\begin{aligned}\overline{C} &= \beta^2 L^d \left[\overline{\langle e^2\rangle} - \overline{\langle e\rangle^2}\right] \\ &= \underbrace{\beta^2 L^d \left[\overline{\langle e^2\rangle} - \overline{\langle e\rangle}^2\right]}_{=C_1} - \underbrace{\beta^2 L^d \left[\overline{\langle e\rangle^2} - \overline{\langle e\rangle}^2\right]}_{=C_2}. \end{aligned} \quad (18)$$

The scaling behavior of C_2 cannot be deduced from the ratio R_e defined by Eq. 12. In contrast to the magnetic sector, R_e vanishes in the thermodynamic limit, meaning that the energy density becomes a self-averaging quantity. Both C_1 and C_2 display a behavior with temperature very different from the average specific heat. In contrast to $\overline{C}$, they diverge in the Griffiths phase and, because of the β^2 prefactor, they keep on growing as the temperature is decreased. We have tested the Finite-Size Scaling of C_1 at several temperatures in the Griffiths phase. While the specific heat is almost independent of the lattice size, C_1 diverges algebraically with a large exponent $(\alpha/\nu)^*$. As shown in Tables IX and X, $(\alpha/\nu)^*$ depends only on the disorder correlation exponent a, and therefore on y, but not on the number of states q, the strength of disorder r, nor the temperature. The estimates are in good agreement with $d - a$ which means that the energy fluctuations are controlled by the disorder fluctuations. This result implies that a strong coupling J_2 essentially freezes the relative state of the two spins, while a weak one J_1 leads to an irrelevant constraint between them. Amazingly, the ratio C_1/C_2 goes to a constant in excellent agreement with 1 for all temperatures in the Griffiths phase. As a consequence, the dominant contributions of C_1 and C_2 cancel out exactly, leading to an algebraic behavior of the specific heat with a much smaller exponent $\alpha/\nu \ll (\alpha/\nu)^*$ than both C_1 and C_2. Since $\alpha/\nu \leq 0$, the largest scaling correction of C_1 and C_2 decays faster than $L^{-(\alpha/\nu)^*}$. In the case of uncorrelated disorder, the ratio C_1/C_2 goes to a value different from 1, even though error bars increase rapidly at large lattice sizes and finally include 1. The cancellation does not take place and the equality $\alpha/\nu = (\alpha/\nu)^*$ is expected.

In the magnetic sector, the exponent $(\gamma/\nu)^*$ was shown to satisfy the hyperscaling relation $(\gamma/\nu)^* = d - 2\beta/\nu = d - 2x_\sigma$ with the exponent β/ν. Assuming that this is also the case in the energy sector, $(\alpha/\nu)^*$ is conjectured to satisfy the hyperscaling relation $(\alpha/\nu)^* = d - 2x_\varepsilon$ where x_ε is the energy scaling dimension. As discussed above, $(\alpha/\nu)^*$ is compatible with $d - a$ which implies $x_\varepsilon = a/2$, i.e. the energy-energy correlation functions, decaying as r^{-2x_ε}, are determined by the coupling correlations in the Griffiths phase.

Finally, the same procedure is applied to the quantity

$$\begin{aligned} -\frac{d}{d\beta}\ln\overline{\langle m\rangle} &= L^d \frac{\overline{\langle me\rangle - \langle m\rangle\langle e\rangle}}{\overline{\langle m\rangle}} \\ &= \underbrace{L^d \frac{\overline{\langle me\rangle} - \overline{\langle m\rangle}\ \overline{\langle e\rangle}}{\overline{\langle m\rangle}}}_{=X_1} - \underbrace{L^d \frac{\overline{\langle m\rangle\langle e\rangle} - \overline{\langle m\rangle}\ \overline{\langle e\rangle}}{\overline{\langle m\rangle}}}_{=X_2} \end{aligned} \quad (19)$$

Both terms in the second line diverge algebraically in the Griffiths phase. Like the specific heat, the exponent $1/\nu^*$ extracted from this divergence does not depend on the number of states q, the strength of disorder r, nor the temperature but only on disorder correlations, i.e. on y or equivalently on a. As can be observed in Tab. XI and XII, the numerical estimates are compatible with $1/\nu^* = d - a/2$. Interestingly, the exponents $(\alpha/\nu)^*$ and $1/\nu^*$ are compatible with the hyperscaling relation

$$\left(\frac{\alpha}{\nu}\right)^* = \frac{2}{\nu^*} - d. \quad (20)$$

This relation is of course exactly satisfied by the two conjectures $(\alpha/\nu)^* = d - a$ et $1/\nu^* = d - a/2$. Assuming $1/\nu^* = d - x_\varepsilon$, the same value of the energy scaling dimension, i.e. $x_\varepsilon = a/2$, is obtained. The ratio X_1/X_2 is compatible with the value 1 at all temperatures in the Griffiths phase. Therefore, the dominant contributions of X_1 and X_2 cancel out, which explains the very different exponent $1/\nu \ll 1/\nu^*$ with which the difference $-\frac{d}{d\beta}\ln\overline{\langle m\rangle} = X_1 - X_2$ diverge. We note that the correction exponent $\omega = 1/\nu^* - 1/\nu$ that is responsible for

TABLE IX. Critical exponent $(\alpha/\nu)^*$ estimated from the Finite-Size Scaling of the quantity C_1 at the self-dual point $\beta_c = 1$. No extrapolation is needed in this case.

y	0	0.25	0.5	0.75	1	1.25	Uncorr. Dis.
$q = 2$, $r = 2$	1.75(2)	1.73(2)	1.68(2)	1.61(2)	1.51(2)	1.35(3)	0.23(6)
$q = 2$, $r = 3$	1.748(11)	1.730(12)	1.681(13)	1.608(14)	1.506(15)	1.35(2)	0.18(6)
$q = 4$, $r = 4$	1.749(9)	1.731(10)	1.682(10)	1.610(11)	1.507(12)	1.34(2)	0.28(5)
$q = 8$, $r = 6$	1.749(8)	1.729(9)	1.681(9)	1.609(9)	1.506(12)	1.343(14)	0.26(5)
$q = 8$, $r = 7.5$	1.748(8)	1.730(8)	1.681(9)	1.608(10)	1.505(11)	1.344(14)	0.21(5)
$q = 8$, $r = 9$	1.747(8)	1.729(8)	1.680(9)	1.607(10)	1.503(11)	1.340(13)	0.18(5)
$q = 16$, $r = 10$	1.747(8)	1.731(9)	1.681(9)	1.606(9)	1.502(10)	1.341(13)	0.20(5)
$d - a$	1.75	1.714	1.667	1.600	1.500	1.333	0

TABLE X. Critical exponent $(\alpha/\nu)^*$ estimated from the Finite-Size Scaling of the quantity C_1 at different temperatures in the Griffiths phase. No extrapolation is needed in this case.

y	0	0.25	0.5	0.75	1	1.25
$q = 2$, $\beta = 1$	1.748(11)	1.730(12)	1.681(13)	1.608(14)	1.506(15)	1.35(2)
$q = 2$, $\beta = 1.2$	1.748(12)	1.730(12)	1.682(13)	1.606(14)	1.51(2)	1.34(2)
$q = 8$, $\beta = 0.75$	1.749(8)	1.731(8)	1.684(9)	1.609(10)	1.506(10)	1.342(13)
$q = 8$, $\beta = 1$	1.748(8)	1.730(8)	1.681(9)	1.608(10)	1.505(11)	1.344(14)
$q = 8$, $\beta = 1.5$	1.747(8)	1.729(9)	1.680(9)	1.605(10)	1.503(11)	1.338(14)
$q = 8$, $\beta = 2$	1.747(8)	1.730(9)	1.680(10)	1.605(10)	1.503(12)	1.340(14)

such a large difference is not an integer, i.e. the largest correction is not analytic, and depends on the disorder correlation exponent a. It is however smaller than for the specific heat.

VI. CONCLUSIONS

A Potts model with algebraically-decaying coupling correlations is studied by large-scale Monte Carlo simulations. Such a disorder is obtained by coupling the polarization density of a quenched self-dual Ashkin-Teller model to the energy density of the Potts model. By construction, the disorder is not generated by a Gaussian action and therefore, multiple-point correlation functions are not trivially given by the Wick theorem. As a consequence, the model is outside of the scope considered by Weinrib and Halperin in the case of the $O(n)$-model. Our model shares two important similarities with the McCoy-Wu model: a Griffiths phase occurs in a finite range of temperatures around the self-dual point and the critical exponents are independent of the number of Potts states q. In contrast to energy, magnetization is shown to be non self-averaging in the Griffiths phase. Magnetization and magnetic susceptibility display algebraic behaviors with the lattice size at all temperatures in the phase Griffiths phase. The exponent β/ν does not depend on the number of Potts states q nor the strength of disorder r but varies with the disorder correlation exponent a and the temperature in the Griffiths phase. Our estimates of γ/ν show a small violation of the hyperscaling relation. This violation is shown to be caused by the exact cancellation of two terms, χ_1 and χ_2, whose difference gives the average susceptibility, as in the 3D Random-Field Ising model. Such a mechanism leads to an hyperscaling violation unless the largest correction of any of the two terms χ_1 or χ_2 diverge only logarithmically. From the scaling of χ_1 and χ_2, an exponent $(\gamma/\nu)^*$ satisfying the hyperscaling relation can be extracted. Because the specific heat does not diverge, the exponent α/ν is negative or zero. However, it can also be written as the difference of two diverging terms. From them, an exponent $(\alpha/\nu)^*$ is defined and shown to be compatible with $d - a$ for any number of Potts state and any temperature in the Griffiths phase. Because the same mechanism than in the magnetic sector takes place, the energy scaling dimension is conjectured to be given by $(\alpha/\nu)^* = d - 2x_\varepsilon$ which implies $x_\varepsilon = a/2$. The exponent ν is extracted from the Finite-Size Scaling of $\frac{d}{d\beta}\overline{\langle m\rangle}$ at different temperatures of the Griffiths phase. Again, this quantity can be written as a difference of two terms, diverging with a much larger exponent $1/\nu^*$ compatible with $d - a/2$, again for any number of Potts states and any temperature in the Griffiths phase.

ACKNOWLEDGMENTS

The author is grateful to Sreedhar Dutta for warm discussions and to the Indian Institute for Science Ed-

TABLE XI. Critical exponent $1/\nu^*$ extrapolated from the Finite-Size Scaling of the quantity X_1 at the self-dual point $\beta_c = 1$.

y	0	0.25	0.5	0.75	1	1.25	Uncorr. Dis.
$q = 2$, $r = 2$	1.88(5)	1.87(6)	1.85(6)	1.82(5)	1.77(6)	1.70(7)	1.00(7)
$q = 2$, $r = 3$	1.88(4)	1.87(4)	1.84(4)	1.82(4)	1.76(5)	1.68(6)	0.97(10)
$q = 4$, $r = 4$	1.88(3)	1.86(3)	1.84(3)	1.80(3)	1.75(3)	1.66(4)	1.08(10)
$q = 8$, $r = 6$	1.88(3)	1.86(3)	1.84(3)	1.81(3)	1.75(3)	1.66(4)	1.10(10)
$q = 8$, $r = 7.5$	1.88(2)	1.87(2)	1.84(2)	1.80(3)	1.75(3)	1.66(4)	1.09(10)
$q = 8$, $r = 9$	1.88(2)	1.87(3)	1.84(3)	1.80(3)	1.75(3)	1.67(4)	1.08(10)
$q = 16$, $r = 10$	1.87(3)	1.86(2)	1.84(2)	1.80(3)	1.75(3)	1.66(3)	1.09(10)
$d - a/2$	1.875	1.857	1.835	1.8	1.75	1.667	1

TABLE XII. Critical exponent $1/\nu^*$ extrapolated from the Finite-Size Scaling of the quantity X_1 at different temperatures in the Griffiths phase.

y	0	0.25	0.5	0.75	1	1.25
$q = 2$, $\beta = 1$	1.88(4)	1.87(4)	1.84(4)	1.82(4)	1.76(5)	1.68(6)
$q = 2$, $\beta = 1.2$	1.91(4)	1.90(4)	1.86(5)	1.82(5)	1.79(5)	1.61(7)
$q = 8$, $\beta = 0.75$	1.86(3)	1.86(2)	1.83(3)	1.80(2)	1.74(3)	1.66(3)
$q = 8$, $\beta = 1$	1.88(2)	1.87(2)	1.84(2)	1.80(3)	1.75(3)	1.66(4)
$q = 8$, $\beta = 1.5$	1.89(3)	1.88(3)	1.85(3)	1.82(3)	1.76(3)	1.67(4)
$q = 8$, $\beta = 2$	1.89(3)	1.88(3)	1.86(3)	1.82(3)	1.77(4)	1.60(5)

ucation and Research (IISER) of Thiruvananthapuram where part of this work was done.

[1] A. B. Harris *J. Phys. C: Solid State Phys.* **7** 1671 (1974).

[2] J.L. Cardy, and J.L. Jacobsen *Phys. Rev. Lett.* **79** 4063 (1997), J.L. Jacobsen, and J.L. Cardy *Nucl. Phys. B* **515** 701 (1998), C. Chatelain, and B. Berche *Nucl. Phys. B* **572** 626 (2000).

[3] A.W.W. Ludwig *Nucl. Phys. B* **285** 97 (1987), A.W.W. Ludwig, and J.L. Cardy *Nucl. Phys. B* **285** 687 (1987), Vl.S. Dotsenko, M. Picco, and P. Pujol *Phys. Lett. B* **347** 113 (1995), Vl.S. Dotsenko, M. Picco, and P. Pujol *Nucl. Phys. B* **455** 701 (1995).

[4] B.N. Shalaev *Sov. Phys. Solid State* **26** 1811 (1984), B.N. Shalaev *Phys. Rep.* **237** 129 (1994), A.W.W. Ludwig *Phys. Rev. Lett.* **61** 2388 (1988), R. Shankar *Phys. Rev. Lett.* **61** 2390 (1988).

[5] A. Pelissetto, and E. Vicari *Phys. Rev. B* **62** 6393 (2000), P. Calabrese, V. Martín-Mayor, A. Pelissetto, and E. Vicari *Phys. Rev. E* **68** 036136 (2003), H.G. Ballesteros, L.A. Fernández, V. Martín-Mayor, A. Muñoz Sudupe, G. Parisi, and J.J. Ruiz-Lorenzo *Phys. Rev. B* **58** 2740 (1998), P.-E. Berche, C. Chatelain, B. Berche and W. Janke *Eur. Phys. J. B* **38** 463 (2004), A.K. Murtazaev, I.K. Kamilov, and A. B. Babaev *Journal of Experimental and Theoretical Physics* **99** 1201 (2004).

[6] Y. Imry and M. Wortis *Phys. Rev. B* **19** 3580 (1979).

[7] K. Hui and A.N. Berker *Phys. Rev. Lett.* **62** 2507 (1989); K. Hui and A.N. Berker *Phys. Rev. Lett.* **63** 2433 (1989).

[8] M. Aizenman and J. Wehr *Phys. Rev. Lett.* **62** 2503 (1989); M. Aizenman and J. Wehr *Comm. Math. Phys.* **130** 489 (1990).

[9] S. Chen, A.M. Ferrenberg and D. P. Landau *Phys. Rev. Lett.* **69** 1213 (1992); S. Chen, A.M. Ferrenberg, and D. P. Landau *Phys. Rev. E* **52** 1377 (1995).

[10] C. Chatelain, and B. Berche *Phys. Rev. Lett.* **80** 1670 (1998). T. Olson, and A.P. Young *Phys. Rev. B* **60** 3428 (1999), C. Chatelain, and B. Berche *Phys. Rev. E* **60** 3853 (1999), J.L. Jacobsen, and M. Picco *Phys. Rev. E* **61** R13 (2000).

[11] H. G. Ballesteros, L. A. Fernández, V. Martín-Mayor, A. Muñoz Sudupe, G. Parisi, and J. J. Ruiz-Lorenzo *Phys. Rev. B* **61** 3215 (2000)

[12] C. Chatelain, B. Berche, W. Janke, and P.-E. Berche *Phys. Rev. E* **64** 036120 (2001), C. Chatelain, B. Berche, W. Janke, and P.-E. Berche *Nucl. Phys. B* **719** 275 (2005).

[13] M.T. Mercaldo, J.-Ch. Anglès d'Auriac, and F. Iglói *Europhys. Lett.* **70** 733 (2005), M.T. Mercaldo, J.-Ch. Anglès d'Auriac, and F. Iglói *Phys. Rev. E* **73** 026126 (2006).

[14] A. Weinrib, and B.I. Halperin *Phys. Rev. B* **27** 413 (1983).

[15] J. Honkonen, and M.Y. Nalimov *J. Phys. A* **22** 751 (1989).

[16] H. G. Ballesteros, and G. Parisi *Phys. Rev. B* **60** 12912 (1999), D. Ivaneyko, B. Berche, Y. Holovatch, and J. Ilnytskyi *Physica A* **387** 4497 (2008).

[17] M.A. Rajabpour and R. Sepehrinia *J. Stat. Phys.* **130** 815 (2008).

[18] R. Sknepnek and T. Vojta *Phys. Rev. B* **69**, 174410 (2004).

[19] B.M. McCoy and T.T. Wu *Phys. Rev.* **176** 631 (1968); B.M. McCoy and T.T. Wu *Phys. Rev.* **188** 982 (1969).

[20] D.S. Fisher *Phys. Rev. B* **51** 6411 (1995).

[21] H. Rieger and F. Iglói *Phys. Rev. Lett.* **83**, 3741 (1999)

[22] F.A. Bagaméry, Loïc Turban, and F. Iglói *Phys. Rev. B* **72** 094202 (2005).

[23] J-Ch. Anglès d'Auriac and F. Iglói *Phys. Rev. Lett.* **90** 190601 (2003); M.T. Mercaldo, J-Ch. Anglès d'Auriac and F. Iglói *Phys. Rev. E* **69** 056112 (2004).

[24] R.B. Griffiths *Phys. Rev. Lett.* **23**, 17 (1969)

[25] T. Vojta *J. Phys. A* **39**, R143 (2006)

[26] T. Senthil and S.N. Majumdar *Phys. Rev. Lett.* **76** 3001 (1996).

[27] E. Carlon, C. Chatelain and B. Berche *Phys. Rev. B* **60** 12974 (1999).

[28] P.-E. Berche, C. Chatelain and B. Berche *Phys. Rev. Lett.* **80** 297 (1998), C. Chatelain, P.-E. Berche, and B. Berche *Eur. Phys. J. B* **7** 439 (1999), D. Girardi, and N.S. Branco *Phys. Rev. E* **83** 061127 (2011).

[29] C. Chatelain *Eur. Phys. Lett.* **102** 66007 (2013).

[30] R. B. Potts *Math. Proc. Camb. Phil. Soc.***48** 106 (1952), F. Y. Wu *Rev. Mod. Phys.***54**235 (1982), F. Y. Wu *Rev. Mod. Phys.***55**315 (1982).

[31] R.H. Swendsen, and J.S. Wang *Phys. Rev. Lett.* **58** 86 (1987).

[32] J. Ashkin et E. Teller *Phys. Rev.* **64** 178 (1943), C. Fan (1972) *Phys. Lett. A* **39** 136.

[33] C. Fan *Phys. Rev. B* **6** 902 (1972).

[34] L. P. Kadanoff *Phys. Rev. Lett.* **39** 903 (1977), L. P. Kadanoff, and A. C. Brown *Annals of Physics* **121** 318 (1979).

[35] J. Salas and A.D. Sokal *J. Stat. Phys.* **85** 297 (1996).

[36] S. Wiseman, and E. Domany *Phys. Rev. E* **52** 3469 (1995).

[37] A. Aharony and A.B. Harris *Phys. Rev. Lett.* **77**, 3700 (1996).

[38] C. Chatelain, B. Berche, and L.N. Shchur *J. Phys. A* **34** 9593 (2001).

[39] Errors on the derivative $\frac{d}{d\beta}\ln\overline{\langle m\rangle}$ were considerably improved compared to Ref. [29]. As discussed in the latter reference, this derivative is computed as the difference of two observables, $\overline{\langle me\rangle}$ and $\overline{\langle m\rangle\langle e\rangle}$, which are several orders of magnitude larger than their difference. If these two observables are computed separately, as it was the case in Ref. [29], it is natural to estimate the error on their difference as the sum of their respective errors. However, this does not reflect the true error on the difference $\bar{X} = \overline{\langle me\rangle} - \overline{\langle m\rangle\langle e\rangle}$ because the two are correlated. The difference was therefore computed during the simulation and the error, estimated by $\sqrt{(\overline{X^2} - \overline{X}^2)/N}$ where N is the number of disorder configuration.

[40] M. Schwartz, and A. Soffer *Phys. Rev. Lett.* **55** 2499 (1985).

[41] A.J. Bray, and M.A. Moore *J. Phys. C* **18** L927 (1985).